Progress in Natural Science: Materials International 36 (2026) 205–214

HOSTED BY

Contents lists available at ScienceDirect

Progress in Natural Science: Materials International

journal homepage: www.elsevier.com/locate/pnsmi

Atomic understanding of effect of rhenium on thermomechanical fatigue properties of Ni-based single crystal superalloys

Wenping Wu[a,b,*], Zijun Ding[a], Zhiqi Xue[a], Yuan Gao[c,d], Chao Yu[e], Guozheng Kang[e]

[a] Department of Engineering Mechanics, School of Civil Engineering, Wuhan University, Wuhan, 430072, China
[b] Wuhan University Shenzhen Research Institute, Shenzhen, 518057, China
[c] Railway Architecture Research Institute, China Academy of Railway Science Group Co., Ltd, Beijing, 10081, China
[d] National Key Laboratory of High-speed Railway Track System, Beijing, 100081, China
[e] Applied Mechanics and Structure Safety Key Laboratory of Sichuan Province, School of Mechanics and Aerospace Engineering, Southwest Jiaotong University, Chengdu, 610031, China

ARTICLE INFO

Keywords:
Ni-based single crystal superalloys
Thermomechanical fatigue
Re effects
Dislocation motion
Molecular dynamics simulation

ABSTRACT

In this paper, atomic simulation of the thermomechanical fatigue (TMF) behavior of Ni-based single crystal superalloys has been achieved, and the effect of Rhenium (Re) on the TMF properties are studied by molecular dynamics (MD) simulation. The reasons why 3%Re improving TMF properties of superalloys are explained from an atomic perspective. The results show that adding 3%Re to the superalloys can increase the cyclic stress amplitude and plastic deformation resistance, reduce the dislocation density and plastic strain energy density, and thereby improve the fatigue life of superalloys. The microstructure evolution reveals that the improvement of TMF properties in superalloys mainly depends on the pinning and dragging effects of Re on dislocation motion. Due to the pinning and dragging effects of Re, the stability of microstructure is significantly enhanced, leading to a reduction in plastic deformation and thus improving the TMF mechanical properties and fatigue life of superalloys. The research results will contribute to a deeper understanding of the TMF mechanisms and Re effects of superalloys.

1. Introduction

Ni-based single crystal superalloys are widely used in the manufacture of turbine blades for aero-engines and industrial gas turbines, due to their excellent mechanical properties, including creep resistance, fatigue resistance, and good surface stability [1–3]. During the operation of the aero-engine, as an important hot end component material for manufacturing engine turbine blades, it is often subjected to repeated erosion by high-temperature and high-pressure gases, as well as thermomechanical fatigue (TMF) failure caused by large-scale temperature changes around the blades during engine start-up, shutdown, and shifting processes [4–7]. It is found that the TMF damage of the superalloys is more complex than that of isothermal fatigue (IF) damage, and the fatigue life of the superalloys under TMF loading is also different from that under IF loading [7,8]. When the superalloy is subjected to TMF loading, more cracks will appear with different crack morphologies from IF loading [9]. The stress concentration at the crack tip may also lead to high-density deformation twinning, and cracks can easily propagate along twinning boundaries, resulting in TMF failure of the superalloys [10]. Moreover, the generation and propagation of cracks in the superalloys under TMF loading become easier and faster [11]. These results in more severe damage to the superalloys under TMF loading than under IF loading, ultimately leading to earlier failure of the superalloys [12–14].

To continuously improve the mechanical properties of the superalloys, it has been found that the service behavior of the superalloys can be improved by adding refractory elements such as W, Mo, and Re [15–19]. One of the main signs is that adding only 3% Re element can significantly reduce the creep rate of the superalloys and improve their creep life [20,21]. Therefore, adding Re element to superalloys has become a major sign in the development of the superalloys [22,23]. The effect of Re on the properties of the superalloys is called the “Re effect” in the superalloys [17,20,24]. Early studies have found that the addition of Re can increase the elastic modulus of the γ matrix phase and promote the solid solution strengthening of the superalloys [22], Moreover, adding Re can also delay the coarsening of the γ′ precipitate phase and maintain

* Corresponding author. Department of Engineering Mechanics, School of Civil Engineering, Wuhan University, Wuhan, 430072, China.
E-mail address: wpwu@whu.edu.cn (W. Wu).

https://doi.org/10.1016/j.pnsc.2026.02.001
Received 22 October 2025; Received in revised form 27 January 2026; Accepted 2 February 2026
Available online 11 February 2026

the stability of γ′ precipitate phase structure to make them more regular [25–29]. Wu et al. [20] found that the Re element gradually accumulates in some dislocations and interface dislocation nuclei during the creep process, leading to a decrease in creep rate, and providing direct evidence that matrix elements can migrate to the γ′ precipitate phase. Zhang et al. [30] found that Re can improve the stability of the γ′ precipitate phase, reduce the sensitivity of lattice mismatch to temperature, and decrease the interface energy of the superalloys. Zhao et al. [31] and Shu et al. [32] found that K-W dislocation locks were formed in superalloys containing Re during creep process, this phenomenon inhibits dislocation slip and cross slip, resulting in better creep resistance of superalloys containing Re. Wang et al. [33] reported that the deformation mechanism of superalloys containing Re under IF loading will gradually change from plane slip to wavy slip with increasing temperature. These studies indicated that the addition of Re to the superalloys has a significant impact on their creep and fatigue properties. However, the current research mainly focuses on the influence of adding Re on the creep and IF properties of the superalloys [19–27,31–35], while the effect of Re on the TMF properties of the superalloys is still unclear.

The TMF properties are closely related to the microstructure evolution mechanisms under TMF loading [36,37]. Due to extremely high cost and difficulties in observing the entire process of microstructure evolution through in-situ experiments for TMF loading, it is necessary to combine numerical simulation to analyze the microstructure evolution and deformation mechanisms of superalloys [38]. Molecular dynamics (MD) simulation has unique advantages in studying the microstructural evolution of materials. It can not only explore the mechanical properties of superalloys under various loading conditions but also observe the entire process characteristics of microstructure evolution and deformation mechanisms of superalloys at the atomic scale, which is of great significance for studying the mechanical properties of superalloys [39–47]. Therefore, in the present study, the mechanical properties of superalloys with and without Re under TMF loading are investigated by MD simulation. The effects of Re on the fatigue mechanical properties and microstructure evolution characteristics of the superalloys under TMF loading are analyzed at the atomic scale. From the view of microstructure evolution, the reason why Re affects the TMF mechanical properties of superalloys is explained, it will contribute to a deeper and better understanding of TMF mechanical properties of superalloys and the microscopic mechanism of Re effects.

2. Modeling and simulation

Ni-based single crystal superalloys are composed of a face-centered cubic (FCC) structure of the γ matrix phase (mainly composed of Ni) and a $L1_2$ structure of the γ′ precipitate phase (mainly composed of Ni_3Al), in which the γ′ precipitate phase is orderly embedded in the γ matrix phase [47,48]. Considering that the second-generation commercial superalloys CMSX-4 has added 3% Re element in comparison to the first-generation superalloys [49,50], in this work, the atomic models of Ni-based single crystal superalloys without Re addition and with 3% Re (3% is the volume fraction) are established using the open-source MD simulation software LAMMPS [51]. To clearly display the interfacial microstructure and dislocation motion characteristics of superalloys during TMF loading, and to endow real geometric morphology of superalloys and physical processes of microstructure evolution, the atomic model adopts three-dimensional (3D) cubic structural units and ensures that the volume fraction of γ′ precipitate phase accounts for about 70%, which is similar to the structure and volume fraction of actual materials. In the atomic model without Re addition, the γ matrix phase is composed of Ni, and the lattice constant $a_\gamma = 3.52$ Å. Whereas γ′ precipitate phase is composed of Ni_3Al with the lattice constant of $a_{\gamma'} = 3.62$ Å. Based on the coincidence site lattice (CSL) $na_{\gamma'} = (n+1)a_\gamma$ on the misfit phase interface, it can be obtained that $n \approx 35$ [47,52]. This means that Ni_3Al of the 35-fold lattice has almost the same volume as Ni of the 36-fold lattice, so replacing 36 × 36 × 36 Ni with 35 × 35 × 35 Ni_3Al in the center of the 40 × 40 × 40 γ matrix model to obtain an ideal atomic model for Ni-based single crystal superalloys without Re addition, as shown in Fig. 1(a). The size of the atomic model is 140.8 Å × 140.8 Å × 140.8 Å, the volume fraction of the γ′ precipitate phase is 72.9%, which is consistent with the volume fraction of the γ′ precipitate phase in the actual Ni-based single crystal superalloys with optimal mechanical properties [48,49,53]. Owing to the propensity of Re atoms to distribute within the γ matrix phase [3,54–57]% volume fraction of Re atoms are randomly added to the γ matrix phase using the same modeling method to create a Ni-based single crystal superalloy atomic model with 3% Re. Therefore, this study aims to investigate the effect of adding 3% Re on TMF mechanical properties in nickel based single crystal superalloys, as illustrated in Fig. 1(b). The superalloys atomic model established in this way is similar to the representative volume element (RVE) in micromechanics, such 3D atomic model can accurately reflect the mechanical properties and microstructural evolution characteristics of superalloys under complex loads [21,40,43–47]. To get rid of the boundary effects, the periodic boundary conditions are applied along the X, Y, and Z directions, and an isothermal-isobaric ensemble (NPT ensemble) is used to control the temperature and pressure of the entire system. The Ni-Al-Re alloy potential [58] is used in the present MD simulation, which has been successfully applied to the study of mechanical properties of the superalloys containing Re element [18,21,45,59]. The initial model is relaxed for 1000ps at 1 K to minimize the model energy and reach a stable state. The common neighbor analysis (CNA) [60] and the dislocation extraction algorithm (DXA) [61] are used to analyze the microstructural evolution characteristics of superalloys under TMF loading, and the OVITO program [62] is used for visualization.

During TMF loading, the temperature fluctuates with the mechanical load variations in each cycle, the two most representative types of TMF are In-phase TMF (IP-TMF) and Out-of-phase TMF (OP-TMF) [13,47,63,64]. In the process of TMF loading, the temperature cycle range is from 300 K to 1200 K, which is consistent with our previous research [47]. The selection of this temperature cycle range not only meets the minimum test temperature close to the room temperature environment, avoiding non conservative results [47,59,64], but also approaches the high-temperature service environment of aircraft engines [65]. First, the sample is gradually heated from 1 K to 750 K without applying

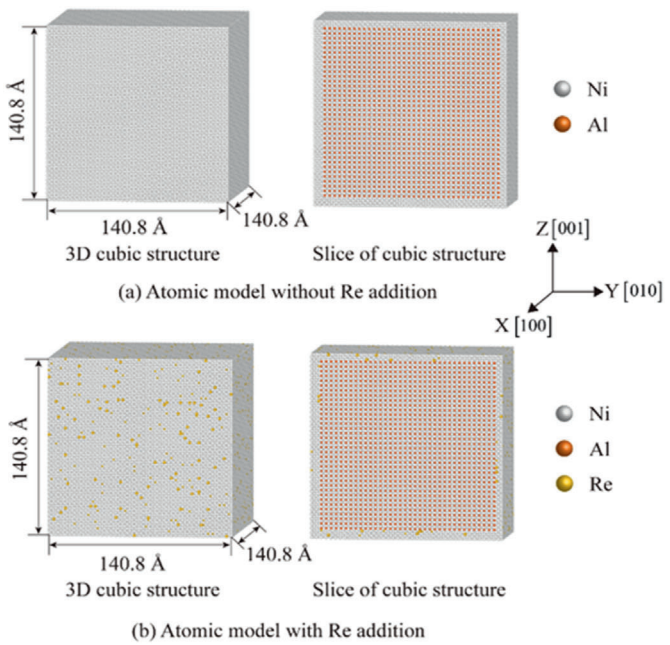

Fig. 1. Three-dimensional cubic Ni-based single crystal superalloy atomic model based on MD simulation. (a) Atomic model without Re addition, (b) Atomic model with Re addition.

mechanical load, and then the sample is relaxed for 50 ps again to minimize the energy and reach a stable state. Subsequently, the mechanical load and temperature are changed simultaneously during the TMF loading process. The triangular waveform loading with a period of 120 ps is applied, and the total number of simulated cycles is $N = 30$. By utilizing the "fix deform" command in the Lammps software to regulate the length of the sample in the Z direction, it is possible to achieve strain loading of the sample. Furthermore, the lengths of the X and Y directions keep nearly constant throughout the loading process. The periodic strain $\frac{\Delta\varepsilon}{2} = 3.0\%$, strain cyclic characteristic coefficient $R = \frac{\varepsilon_{min.}}{\varepsilon_{max}} = -1$, and the strain rate $\dot{\varepsilon} = 1.0 \times 10^9/\mathrm{s}$ is applied along the Z direction, while no load is applied in the X and Y directions. During the IP-TMF loading process, both the temperature and the mechanical load increase and decrease simultaneously. During each cycle, when the mechanical load increases from $\varepsilon = 0\%$ to $\varepsilon = 3\%$, the temperature increases from 750 K to 1200 K. Then, as the mechanical load decreases from $\varepsilon = 3\%$ to $\varepsilon = -3\%$, the temperature also decreases from 1200 K to 300 K. Finally, when the mechanical load changes from $\varepsilon = -3\%$ to $\varepsilon = 0\%$, the temperature increases from 300 K to 750 K, as shown in Fig. 2(a). During the OP-TMF loading process, there is a phase difference of 180° between the mechanical load and the temperature. During each cycle, when the mechanical load increases from $\varepsilon = -3\%$ to $\varepsilon = 3\%$, the temperature decreases from 1200 K to 300 K. Conversely, when the mechanical load increases from $\varepsilon = 3\%$ to $\varepsilon = -3\%$, the temperature increases from 300 K to 1200 K, as illustrated in Fig. 2(b).

3. Results and discussion

3.1. Effect of Re on cyclic stress-strain curves

Fig. 3 shows the cyclic stress-strain curves of superalloys with Re and without Re addition under TMF loading to illustrate the effect of Re on the cyclic stress-strain curves. It can be seen from Fig. 3 that the addition of Re does not change the basic cycle characteristics of the superalloys, the cyclic stress-strain curves of the superalloys still exhibit tension-compression asymmetry under TMF loading. Under IP-TMF loading, the maximum tensile stress of the superalloys with and without Re addition is lower than the maximum compressive stress, while under OP-TMF loading, the maximum tensile stress is higher than the maximum compressive stress. The main reasons for the existence of tension-compression asymmetry in Ni-based superalloys under TMF loading can be explained as: (1) For IP-TMF loading case, in the high-temperature stage, compressive stress promotes the directional coarsening of the γ' phase (forming a raft like structure), hinders dislocation movement, and requires higher compressive stress to maintain deformation; In the low-temperature stage, tensile stress acts on the strengthened structure, resulting in a relative decrease in stress. (2) For OP-TMF loading case, the high temperature tensile stress causes local dissolution of the γ' phase, forming softening channels and reducing subsequent compressive stress; low temperature compressive stress acts on the γ matrix (not fully strengthened), requiring higher tensile stress to induce yield. Therefore, the superalloys exhibit tension-compression asymmetry during TMF loading.

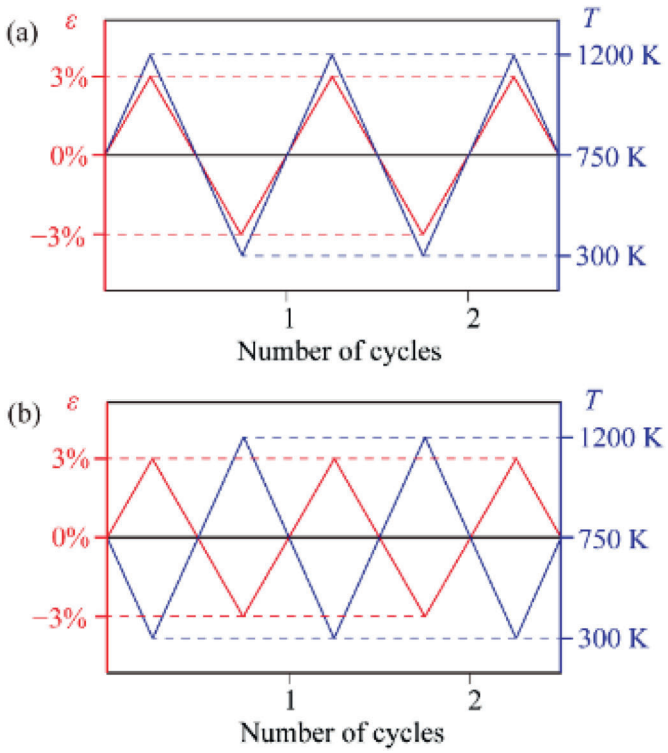

Fig. 2. Schematic diagram of TMF loadings. (a) IP-TMF, (b) OP-TMF.

In addition, it can also be seen from Fig. 3 that the addition of Re can increase the stress range ($\Delta\sigma = \sigma_{max,t} - \sigma_{max,c}$ namely, the difference between the maximum tensile stress and the maximum compressive stress) of the superalloys. Under both IP-TMF and OP-TMF loading conditions, the superalloys with Re addition have a higher stress range ($\Delta\sigma$) than those of superalloys without Re addition. Taking OP-TMF loading as an example, in the 30th cycle, the stress range of the superalloys without Re addition is $\Delta\sigma = 9.86$ GPa, while the stress range of the superalloys with Re addition is $\Delta\sigma = 12.02$ GPa. The cyclic stress-strain curves of the superalloys with Re addition also show a narrower characteristic compared to those of the superalloys without Re addition, which is related to the different plastic work of superalloys with and without Re addition under IP-TMF and OP-TMF loadings.

To verify the accuracy and reliability of the model, the elastic parameters are calculated based on cyclic stress-strain curves through MD simulations and compared with the existing experimental results. Table 1 shows the elastic modulus values of two typical superalloys with and without Re addition. Based on experimental test results from early literature [1], the elastic modulus of the first-generation superalloys without Re addition (PWA1480) is between 143 and 201 GPa within the temperature range of 300–1173K, while the elastic modulus of the second-generation superalloys with Re addition (CMSX-4) is between 160 and 225 GPa at the same temperature conditions. The experimental results in the literature indicate that the addition of Re element increases the elastic modulus of the superalloys. Based on the cyclic stress-strain curves in the current MD simulations, we can obtain the elastic modulus values of superalloys without Re addition in IP-TMF and OP-TMF tests is 168 GPa and 193 GPa, respectively, while the values of superalloys with Re addition is 185 GPa and 217 GPa in IP-TMF and OP-TMF tests, respectively. Overall, whether in IP-TMF or OP-TMF test, the elastic modulus of superalloys with Re addition is higher than that of superalloys without Re addition, which is consistent with the experimental results in the literature [1], and these calculated values of elastic modulus by MD simulations are all within the range of experimental values. These indicate the rationality of the atomic model and potential function used in the present MD simulations.

3.2. Effect of Re on stress response

Fig. 4 shows cyclic stress response curves of samples with Re and without Re under TMF loading. The effect of Re on the cyclic stress response curves of Ni-based single crystal superalloys are analyzed under IP-TMF and OP-TMF loadings. These stress response curves including: (a) maximum tensile stress $\sigma_{max,t}$, (b) maximum compressive stress $\sigma_{max,c}$, (c) cyclic stress amplitude $\sigma_a = \frac{\sigma_{max,t} - \sigma_{max,c}}{2}$, and (d) mean stress $\sigma_m = \frac{\sigma_{max,t} + \sigma_{max,c}}{2}$. It has been found that the superalloys with Re addition has higher maximum tensile stress $\sigma_{max,t}$, maximum

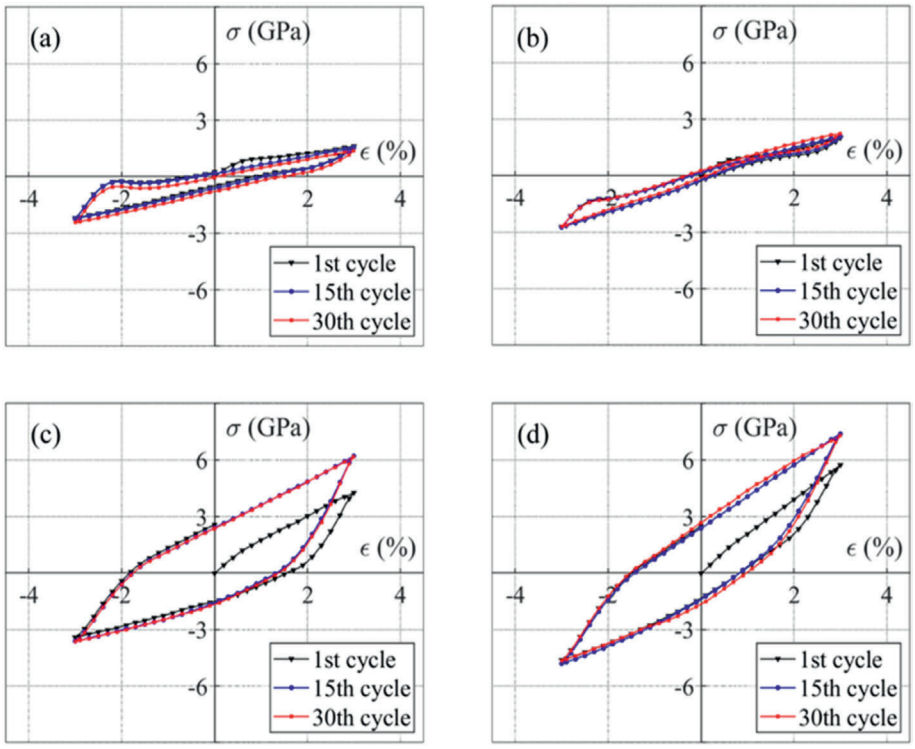

Fig. 3. Effect of Re on the cyclic stress-strain curves of the superalloys under TMF loadings. (a) IP-TMF, without Re addition, (b) IP-TMF, with Re addition, (c) OP-TMF, without Re addition, (d) OP-TMF, with Re addition.

Table 1
Comparison of elastic modulus obtained from experiments and MD simulations.

Generation	Alloys	Re Content (Wt %)	Elastic Modulus (GPa)		
			Room Temperature (300 K) [1]	High Temperature (1173 K) [1]	MD simulations (TMF 300~1200K)
1st Generation (Without Re addition)	PWA1480	0	198 ± 3	145 ± 2	168 (IP-TMF) 193 (OP-TMF)
2nd Generation (With Re addition)	CMSX-4	3	223 ± 2	162 ± 2	185 (IP-TMF) 217 (OP-TMF)

compressive stress $\sigma_{max,c}$, and cyclic stress amplitude σ_a than those of superalloys without Re addition whether in IP-TMF test or OP-TMF test, as shown in Fig. 4 (a) -(c). This indicates that the addition of Re to the superalloys can significantly increase the cyclic stress amplitude of the superalloys under TMF loading, which is consistent with the experimental results of the effect of Re element on the cyclic stress amplitude of the superalloys under low cycle fatigue loading [26,27]. Moreover, there is a higher cyclic stress amplitude in OP-TMF test than that of IP-TMF test, as shown in Fig. 4(c). For the mean stress σ_m, the effect of Re on the σ_m is not significant, only slightly increased. In IP-TMF test, σ_m is manifested as the compressive stress, while it is manifested as the tensile stress in OP-TMF test, as shown in Fig. 4(d), this is consistent with the results in OP-TMF test by Tan et al. [36]. Table 2 lists the specific values of the $\sigma_{max,t}$, $\sigma_{max,c}$, σ_a, σ_m for both the superalloys with Re and without Re addition at the 30th cycle under IP-TMF and OP-TMF loadings. From Table 2 and it further indicates that adding Re can increase the cyclic stress amplitude of the superalloys in TMF test, and Re has a higher effect on the cyclic stress amplitude in OP-TMF test than IP-TMF test.

3.3. Effects of Re on plastic strain energy density and dislocation density

The area of each cyclic hysteresis loop in the cyclic stress-strain curve represents the plastic deformation work per unit volume of each cycle, this area signifies the plastic strain energy density, reflecting the energy dissipation during the loading process and providing insight into the plastic deformation situation [66].

Fig. 5 shows the variation curves of the plastic strain energy density ΔW_p of superalloys with and without Re addition under TMF loading. It is evident that the ΔW_p of the superalloys with Re addition is lower than that of the superalloys without Re addition whether in IP-TMF test or OP-TMF test. This indicates that less energy dissipation and less plastic deformation occur in the superalloys with Re addition than those of the superalloys without Re addition under TMF loading. This is also the reason why the cyclic stress-strain curves of the superalloys with Re addition have narrower characteristics in Fig. 3(b) and (d). In addition, the ΔW_p of the superalloys under OP-TMF loading is significantly higher than that under IP-TMF loading, which reveals that the plastic deformation and energy dissipation of the superalloys under OP-TMF loading are higher than those under IP-TMF loading. This is also the main reason why OP-TMF determines the fatigue performance and fatigue life of superalloys in TMF test.

Fig. 6 shows the variation curves of dislocation density of superalloys with and without Re addition under TMF loading to illustrates the influences of Re on dislocation density and plastic deformation. Due to the interaction of dislocations during the cyclic loading process, when the superalloys reach the cyclic stability stage, the dislocation density tends to be dynamically balanced in both the superalloys with and without Re addition. It can be observed that the addition of Re significantly affects

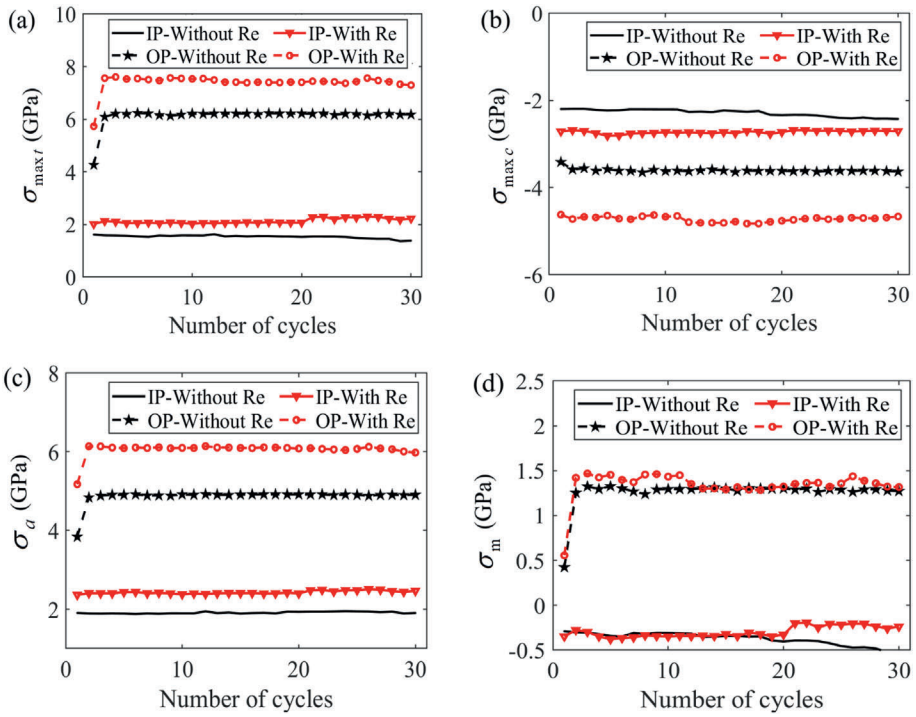

Fig. 4. Effect of Re on the cyclic stress response of the superalloys under TMF loadings. (a) Maximum tensile stress, $\sigma_{max,t}$, (b) Maximum compressive stress, $\sigma_{max,c}$, (c) cyclic stress amplitude σ_a, and (d) mean stress, σ_m.

Table 2
Cyclic stress response and difference value between the superalloys with Re addition and without Re addition at the 30th cycle under TMF loadings.

Loading conditions		$\sigma_{max,t}$ (GPa)	$\sigma_{max,c}$ (GPa)	$\sigma_a = \frac{\sigma_{max,t} - \sigma_{max,c}}{2}$ (GPa)	$\sigma_m = \frac{\sigma_{max,t} + \sigma_{max,c}}{2}$ (GPa)
IP-TMF	Without Re addition	1.45	−2.41	1.93	−0.48
	With Re addition	2.25	−2.73	2.49	−0.24
OP-TMF	Without Re addition	6.24	−3.62	4.93	1.31
	With Re addition	7.35	−4.67	6.01	1.34

the dislocation density of superalloys under TMF loading when the dislocation density reaches the dynamic equilibrium stage. Under both IP-TMF and OP-TMF loading conditions, the superalloys with Re addition exhibits a lower dislocation density than that of superalloys without Re addition. Due to the fact that the volume of superalloys with Re addition is the same as that of superalloys without Re addition, the lower dislocation density also means that there are fewer dislocations in superalloys with Re addition. Therefore, the addition of Re can decrease the number of dislocations in the superalloys, correspondingly, there is less plastic deformation occurring in the superalloys.

3.4. Effect of Re on microstructure evolution

In our previous simulation work [47] and early experimental study on TMF [13,14,67] have indicated that the superalloys have a shorter fatigue life under OP-TMF loading. Therefore, the OP-TMF loading determines the TMF mechanical properties and fatigue life of Ni-based single crystal superalloys, the dislocation motion characteristics of superalloys under OP-TMF loading are chosen to analyze the effect of Re on dislocation motion in superalloys, and the reasons why Re can reduce dislocation density and plastic strain energy density are explored. Fig. 7 shows the characteristics of dislocation motion in superalloys with Re

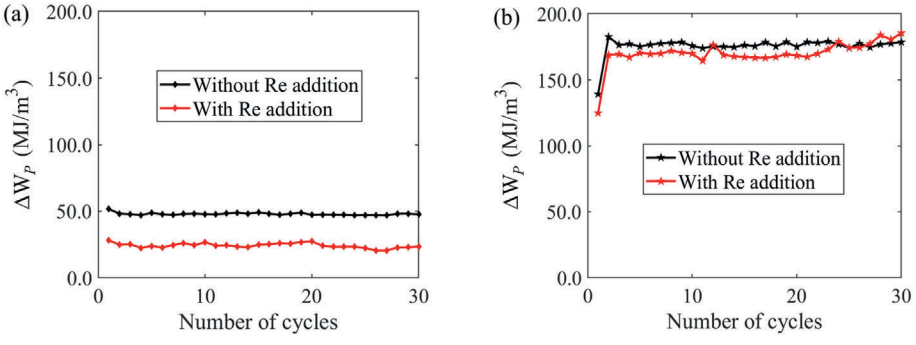

Fig. 5. Effect of Re on the plastic strain energy density of the superalloys under TMF loadings. (a) IP-TMF, (b) OP-TMF.

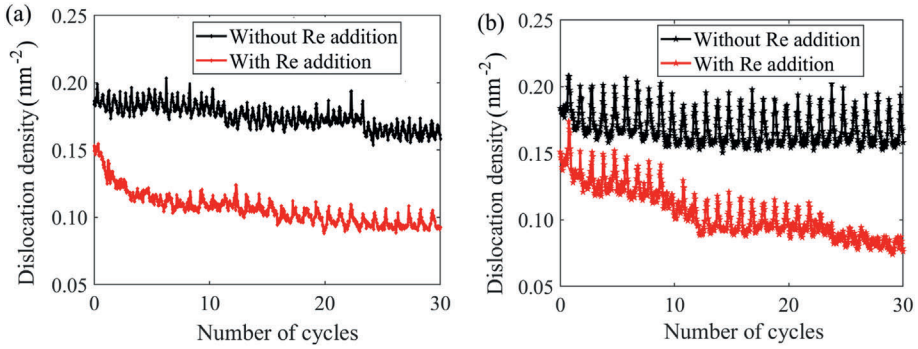

Fig. 6. Effect of Re on the dislocation density of the superalloys under TMF loadings. (a) IP-TMF, (b) OP-TMF.

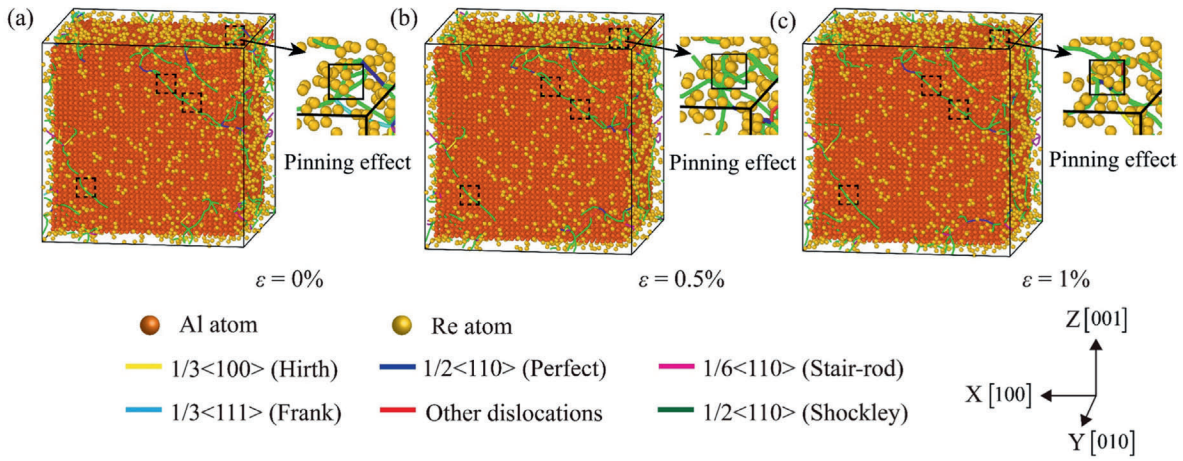

Fig. 7. Re atoms produce pinning effect on the dislocation motion of the superalloys under OP-TMF loadings. (a) $\varepsilon = 0\%$, (b) $\varepsilon = 0.5\%$, (c) $\varepsilon = 1\%$.

addition under OP-TMF loading. In the superalloys with Re addition, the Re atoms are randomly distributed in the γ matrix phase before loading (Fig. 1 (b)).

As the cyclic loading progresses, the Re atoms gradually tend to move to the γ/γ′ interface. At this point, the Re atoms distributed in the γ matrix phase and the γ/γ′ interface will have a pinning effect on the mobile dislocations in the γ matrix phase, and preventing these mobile dislocations from entering the γ′ precipitate phase. As the loading process continues, this pinning effect causes the dislocation motion to be continuously hindered, increasing the resistance of the dislocation to cut into the γ′ precipitate phase. This makes it more difficult for dislocations to cut into the γ′ precipitate phase, resulting in more dislocations concentrated in the γ matrix phase channels and at the γ/γ′ interface. This phenomenon is also well supported by the viewpoint that Re will produce pinning force to hinder dislocation motion [68,69]. In the previous experimental observation, Wu et al. [20] used the Atom probe tomography technique to detect the distribution of Re elements in Ni-based single crystal superalloys containing 3% Re elements during creep. During the loading process, it was observed that the Re element gradually accumulates at the interface dislocation nucleus, which provided good support for Re atoms to gradually tilt from the γ matrix phase towards the γ/γ′ interface and pin interface dislocations.

As the loading process continues, the pinning force of Re atoms on dislocations is insufficient to confine the moving dislocations to the γ matrix phase channel. Consequently, some dislocations have penetrated the γ′ precipitate phase. Additionally, Re atoms tend to be distributed at the γ/γ′ interface, with some Re atoms gradually infiltrating the γ′ precipitate phase [20,21,45]. At this time, the Re atoms that have entered the γ′ precipitate phase in the superalloy sample with Re will have a drag effect on the dislocation motion, as shown in Fig. 8. The drag effect of Re on the dislocation results in a stronger obstacle to the movement of the dislocation in the γ′ precipitate phase. This impedes the movement of the dislocation in the γ′ precipitate phase, making it more challenging to shear the γ′ precipitate phase, which further reduces the occurrence of plastic deformation in the γ′ precipitate phase. In addition, from Fig. 8, it can also be observed that the dislocations in the γ′ precipitate phase of superalloys with Re addition are considerably fewer than those in the superalloys without Re addition, resulting in a significantly lower dislocation density in the superalloys with Re addition. Meanwhile, this lower dislocation density also results in a fewer dislocation shearing the γ′ precipitate phase. This is one of the reasons for the reduction in the plastic deformation in the γ′ precipitate phase of the superalloys with Re addition during TMF loading. In other words, the superalloys with Re addition exhibit a lower plastic strain energy density.

Fig. 9 shows the microstructure evolution characteristics of the superalloys with and without Re during the OP-TMF loading process. Since the model of superalloys used in the present simulation is an atomic model with a three-dimensional cubic structure, only the microstructural evolution characteristics of the γ matrix phase can be observed on the surface of the sample, to clearly observe the microstructure characteristics within the γ′ precipitate phase, a cross-sectional analysis of the samples of superalloys is performed along the X direction to analyze the microstructural characteristics of γ matrix and γ′ precipitate phases. By comparing Fig. 9 (a) and 9 (c), it can be observed that in the superalloys without Re addition, some dislocations and stacking faults (SFs) occur on the surface of the sample (i.e., the γ matrix phase), but these dislocations and SFs in the γ matrix phase gradually decrease as the loading progresses (as the strain increases from 0 to 3%). Moreover, it can be observed from the cross-section of the model that some dislocations have obviously cut into the γ′ precipitate phase, resulting in

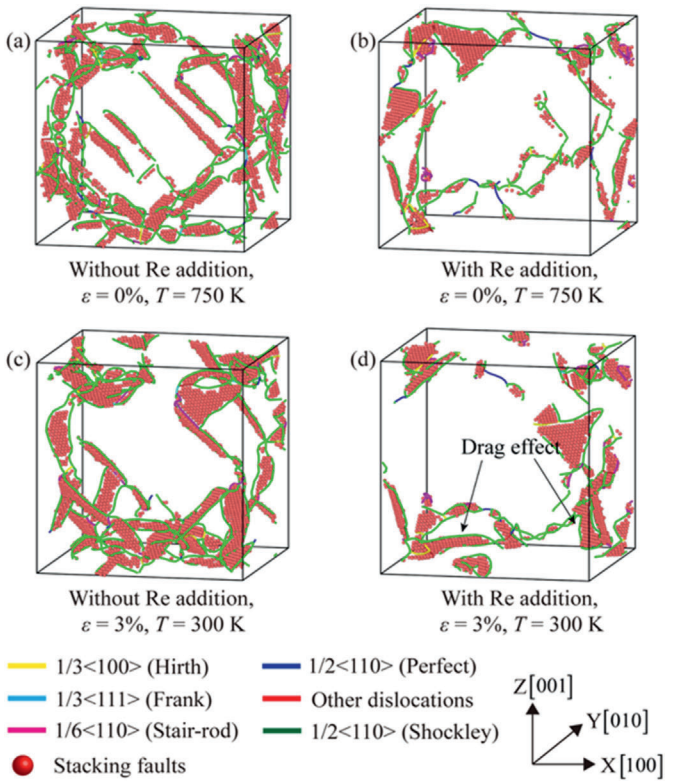

Fig. 8. Re atoms produce dragging effect on the dislocation motion of the superalloys under OP-TMF loadings. (a) Without Re addition, ε = 0%, T = 750 K, (b) With Re addition, ε = 0%, T = 750 K, (c) Without Re addition, ε = 3%, T = 300 K, (d) With Re addition, ε = 3%, T = 300 K.

significant plastic deformation of the γ′ precipitate phase. For the sample of superalloys with Re addition, from the comparison between Fig. 9 (b) and 9 (d), it can be found that the dislocations are mostly confined to the γ matrix phase and the γ/γ′ interface during the loading process, and few dislocations can enter the γ′ precipitate phase. This is due to the pinning effect caused by Re atoms, which continuously hinders the movement of dislocations, increases the resistance of dislocations to enter the γ′ precipitate phase, leading to the dislocations are only concentrated in the γ matrix phase and at the γ/γ′ interface, and unable to enter the γ′ precipitate phase. As the cyclic loading continues, some dislocations break through the pinning force and cut into the γ′ precipitate phase. Re further participates in the drag effect on dislocations to further prevent their movement, although some dislocations γ′ precipitate phase in the later of cycling loading. Therefore, almost no obvious plastic deformation occurs in the γ′ precipitate phase of superalloys with Re addition. This comparison demonstrates that the pinning and dragging effects of Re on dislocation motion effectively impede the movement of dislocations. As a results, the plastic deformation and plastic strain energy density decreases, Correspondingly, the fatigue resistance performance of superalloys with Re addition is enhanced.

It is precisely because of the pinning and dragging effects of Re on the dislocation motion during cyclic loading that dislocation motion is hindered and hardly entered the γ′ precipitate phase, thereby improving the stability of the microstructure and exhibiting less plastic deformation in the γ′ precipitate phase. In addition, the hindrance of dislocation motion in the superalloys with Re addition is attributed to the pinning and dragging effects of Re, which results in higher cyclic stress amplitude in the superalloys with Re addition. The pinning and dragging effects of Re on dislocation motion is well supported by relevant experimental observations [68,69].

3.5. Effects of Re on interface energy and fatigue life

Interface energy, also known as surface energy, describes the energy per unit area at a two-phase interface [70]. According to the definition of interface energy, in Ni-based superalloys, the interface energy can be calculated using the following equation:

$$\kappa_{interface} = \frac{E_{total} - \left(E_{\gamma} + E_{\gamma'}\right)}{2A} \tag{1}$$

where E_{total} refers to the total potential energy of the entire system during the relaxation process of the Ni-based superalloys samples; E_{γ} represents the total potential energy of γ phase in the system; $E_{\gamma'}$ represents the total potential energy of γ′ phase in the system; A represents the area of γ/γ′ interface.

During the calculation process, two Ni-based superalloys samples with 3%Re addition and without Re addition are constructed to calculate the E_{total} and A. Subsequently, the γ phase and γ′ phase with the same composition as the Ni-based superalloys samples are separately constructed to calculate E_{γ} and $E_{\gamma'}$. Fig. 10 shows the changes in interface energy during the relaxation process of Ni-based superalloys with and without Re addition. It can be seen that the addition of Re results in a lower interface energy, indicating that Re can strengthen the interface and make it more stable.

After the sample relaxation is completed, MD simulation is further used to perform TMF loading. Based on the current simulation, the Coffin-Manson equation improved by Ostergren [71] was used to estimate the fatigue life:

$$C_1 = \triangle W_T N_f^{\beta} = \lambda \sigma_{\max\, t} \Delta\varepsilon_p N_f^{\beta} \tag{2}$$

$$C = (C_1 / \lambda) = \sigma_{\max\, t} \Delta\varepsilon_p N_f^{\beta} \tag{3}$$

Where λ, C, C_1 and β are material constants, $\sigma_{\max\, t}$ is the maximum tensile stress, $\Delta\varepsilon_P$ is the plastic strain range, and ΔW_T is tensile hysteretic energy. In equation (3), due to C and β are material constants, they only depend on material properties. Thus, the Ostergren parameter $\sigma_{\max\, t}\Delta\varepsilon_P$ is the determining factor of fatigue life, the larger the value of this Ostergren parameter is, the lower the fatigue life is. Since the cycle has completely entered stable state in the 30th cycle, the data from the 30th cycle in the stable state are selected for calculation, the detailed parameters are shown in Table 3.

As stated previously, the mechanical properties of the superalloys under OP-TMF loading determines the TMF life of Ni-based single crystal superalloys [13,14,47,67]. In this work, the fatigue behaviors of the superalloys with and without Re addition under OP-TMF loading are selected for analysis, it is assumed that the constant values of C and β are identical values in the superalloys with and without Re addition. From Table 3, we can see that the Ostergren parameter $\sigma_{\max\, t}\Delta\varepsilon_P$ (15.29) of superalloys with Re addition is lower than that of superalloys without Re addition (22.15). Therefore, it can be concluded that the superalloys with Re addition has a longer fatigue life than that of superalloys without Re addition, which indicates that the addition of 3%Re can improve the fatigue strength and fatigue life of the superalloys, it has been supported by early experimental results [50].

4. Conclusions

In this study, MD simulation is used to analyze the mechanical properties and microstructural evolution characteristics of Ni-based single crystal superalloys with and without Re addition under TMF loading. The influences of Re on the TMF mechanical properties and microstructure evolution of the superalloys are analyzed. Moreover, the micro-mechanisms of enhancing fatigue resistance and improving the TMF life are explained at atomic scale. The main conclusions are as follows.

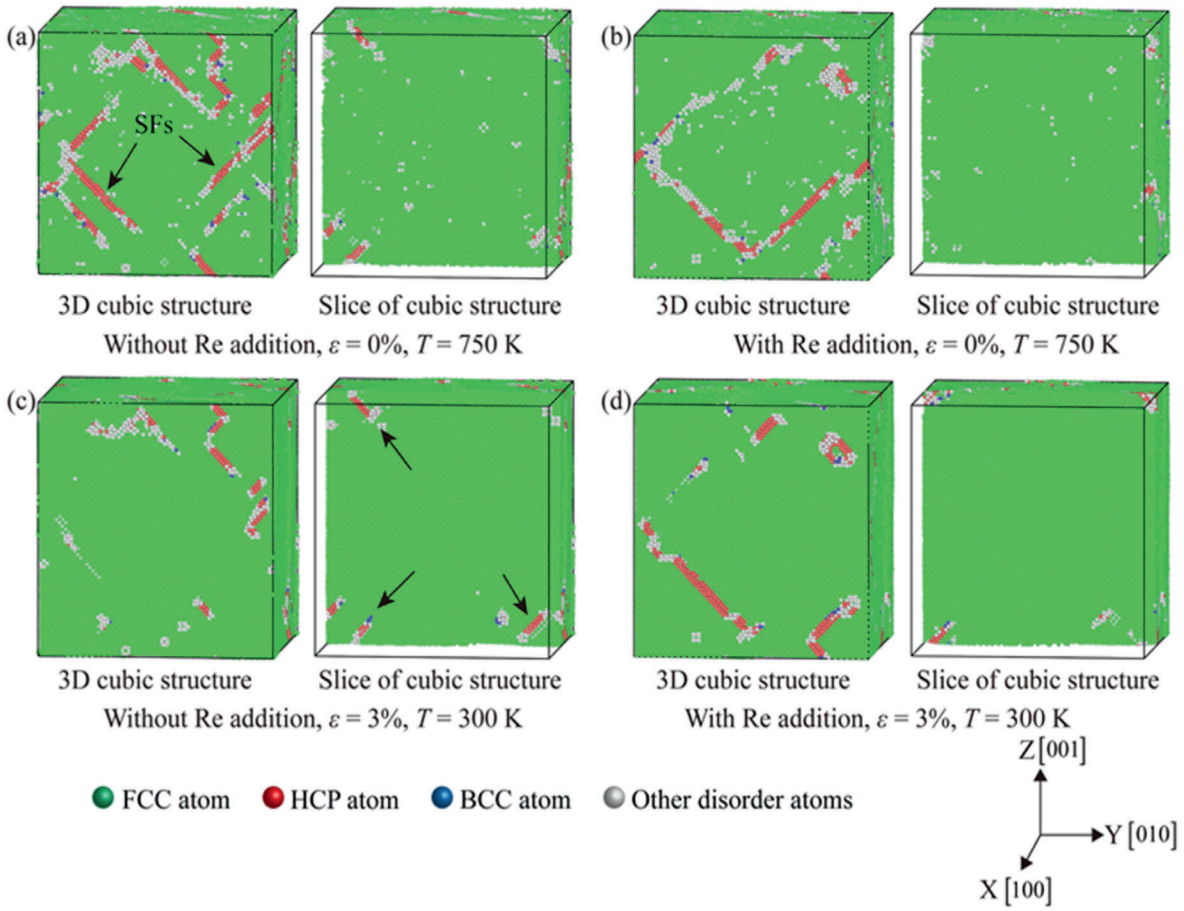

Fig. 9. Microstructure characteristics of the superalloys with and without Re addition under OP-TMF loadings. (a) Without Re addition, ε = 0%, T = 750 K, (b) With Re addition, ε = 0%, T = 750 K, (c) Without Re addition, ε = 3%, T = 300 K, (d) With Re addition, ε = 3%, T = 300 K.

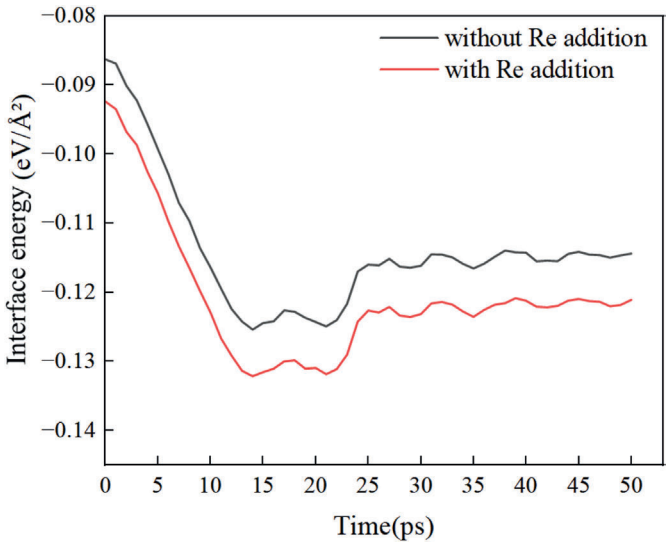

Fig. 10. Changes in interfacial energy during the relaxation process of superalloys with and without Re addition.

(1) Adding 3%Re to Ni-based single crystal superalloys can significantly improve TMF mechanical properties of superalloys, including: increasing the stress range and cyclic stress amplitude, reducing the plastic strain energy density and energy dissipation during TMF loading process, and improving the interface stability and TMF life of superalloys, which are similar to the effect of adding Re on low cycle fatigue performance of superalloys.

(2) Adding 3%Re almost does not change the basic cycle characteristics, but can increase the maximum tensile stress and the maximum compressive stress of the superalloys under TMF loading. The cyclic stress-strain curves of the superalloys still exhibit tension-compression asymmetry under TMF loading. In IP-TMF test, the maximum tensile stress is lower than the maximum compressive stress of the superalloys, while the maximum tensile stress is higher than the maximum compressive stress in OP-TMF test.

(3) Adding 3%Re can improve the TMF mechanical properties and fatigue life of the superalloys mainly depends on the pinning and dragging effects of Re on dislocation motion. In the early stage of cyclic loading, the Re atoms exert a pinning effect on dislocation motion, making it difficult for the dislocations to enter the γ′ precipitate phase. In the later stage of cyclic loading, Re atoms gradually enter the γ′ precipitate phase, which also impedes the movement of dislocations within the γ′ precipitate phase by exerting a dragging effect on the dislocations.

The current atomic model is based on the ideal Ni-Ni_3Al alloy model to analyze the effect of doping with Re atoms on the TMF mechanical properties of the superalloys, effectively explaining the reason why adding Re atoms improves the TMF life of superalloys at the atomic scale. Of course, the real superalloys (such as: CMSX-4) contain more complex elements such as Ni, Al, Re, Cr, W, Ta, Ti, etc. In future

Table 3
Mechanical parameters and predicted fatigue life of the superalloys with and without Re addition under OP-TMF loading.

	Samples	$\Delta\varepsilon$ (%)	$\Delta\varepsilon_p$ (%)	$\sigma_{max,\ t}$ (GPa)	$\sigma_{max,\ c}$ (GPa)	$\Delta\sigma$ (GPa)	$\sigma_{max,t}\ \Delta\varepsilon_p$	Fatigue life
OP-TMF	Without Re	6.0	3.55	6.24	−3.62	9.86	22.15	$\boldsymbol{N_{f\ (with\ Re)} >}$
	With Re	6.0	2.08	7.35	−4.67	12.02	15.29	$\boldsymbol{N_{f\ (without\ Re)}}$

research, atomic models containing more complex doping elements can be further established to deeply explore the influence of doping elements on the mechanical properties of superalloys.

CRediT authorship contribution statement

Wenping Wu: Writing – original draft, Validation, Resources, Funding acquisition, Formal analysis, Data curation, Conceptualization. **Zijun Ding:** Visualization, Validation, Software, Methodology, Investigation, Data curation. **Zhiqi Xue:** Visualization, Validation, Software, Investigation, Data curation. **Yuan Gao:** Validation, Software, Resources, Methodology, Formal analysis. **Chao Yu:** Writing – review & editing, Validation, Methodology, Investigation, Formal analysis, Data curation. **Guozheng Kang:** Writing – review & editing, Validation, Supervision, Software, Project administration, Methodology, Formal analysis, Conceptualization.

Declaration of competing interest

The authors declare that they have no known competing financial interests or personal relationships that could have appeared to influence the work reported in this paper.

Acknowledgements

The authors gratefully acknowledge the financial support provided by the National Natural Science Foundation of China (Grant Nos. 12172259 and 11772236), Guangdong Basic and Applied Basic Research Foundation, China (Grant Nos. 2023A1515012745 and 2024A1515012185), Open Project of National Key Laboratory of High-speed Railway Track System, China (Grant No. 2025YJ180).

References

[1] R.C. Reed, The Superalloys: Fundamentals and Applications, Cambridge university press, 2008.
[2] T.M. Pollock, Alloy design for aircraft engines, Nat. Mater. 15 (8) (2016) 809–815.
[3] M. Shahwaz, P. Nath, I. Sen, A critical review on the microstructure and mechanical properties correlation of additively manufactured nickel-based superalloys, J. Alloys Compd. 907 (2022) 164530.
[4] W.J. Zhang, Thermal mechanical fatigue of single crystal superalloys: achievements and challenges, Mater. Sci. Eng., A 650 (2016) 389–395.
[5] V. Norman, S. Stekovic, J. Jones, M. Whittaker, B. Grant, On the mechanistic difference between in-phase and out-of-phase thermo-mechanical fatigue crack growth, Int. J. Fatig. 135 (2020) 105528.
[6] P. Zhang, Q. Zhu, G. Chen, C.J. Wang, Review on thermo-mechanical fatigue behavior of nickel-base superalloys, Mater. Trans. 56 (12) (2015) 1930–1939.
[7] M. Okazaki, M. Sakaguchi, Thermo-mechanical fatigue failure of a single crystal Ni-based superalloy, Int. J. Fatig. 30 (2) (2008) 318–323.
[8] X. Song, Y. Jiang, X.A. Hu, X.F. Nie, Thermomechanical fatigue and life prediction method of a precision cast superalloy with electrical discharge machining drilled holes, Int. J. Fatig. 166 (2023) 107253.
[9] H.U. Hong, J.G. Kang, B.G. Choi, I.S. Kim, Y.S. Yoo, C.Y. Jo, A comparative study on thermomechanical and low cycle fatigue failures of a single crystal nickel-based superalloy, Int. J. Fatig. 33 (12) (2011) 1592–1599.
[10] J.X. Zhang, H. Harada, Y. Ro, Y. Koizumi, T. Kobayashi, Thermomechanical fatigue mechanism in a modern single crystal nickel base superalloy TMS-82, Acta Mater. 56 (13) (2008) 2975–2987.
[11] R.K. Kersey, A. Staroselsky, D.C. Dudzinski, M. Genest, Thermomechanical fatigue crack growth from laser drilled holes in single crystal nickel-based superalloy, Int. J. Fatig. 55 (2013) 183–193.
[12] Z.W. Huang, Z.G. Wang, S.J. Zhu, F.H. Yuan, F.G. Wang, Thermomechanical fatigue behavior and life prediction of a cast nickel-based superalloy, Mater. Sci. Eng., A 432 (1) (2006) 308–316.
[13] G.M. Han, J.J. Yu, X.F. Sun, Z.Q. Hu, Thermo-mechanical fatigue behavior of a single crystal nickel-based superalloy, Mater. Sci. Eng., A 528 (19) (2011) 6217–6224.
[14] J.Y. Sun, H. Yuan, Life assessment of multiaxial thermomechanical fatigue of a nickel-based superalloy Inconel 718, Int. J. Fatig. 120 (2019) 228–240.
[15] P. Caron, T. Khan, Evolution of Ni-based superalloys for single crystal gas turbine blade applications, Aero. Sci. Technol. 3 (8) (1999) 513–523.
[16] B.H. Ge, Y.S. Luo, J.R. Li, J. Zhu, Distribution of rhenium in a single crystal nickel-based superalloy, Scr. Mater. 63 (10) (2010) 969–972.
[17] H.T. Mallikarjuna, N.L. Richards, W.F. Caley, Effect of alloying elements and microstructure on the cyclic oxidation performance of three nickel-based superalloys, Materialia 4 (2018) 487–499.
[18] R.H. Wu, Q. Yin, J.P. Wang, Q.Z. Mao, X. Zhang, Z.X. Wen, Effect of Re on mechanical properties of single crystal Ni-based superalloys: insights from first-principle and molecular dynamics, J. Alloys Compd. 862 (2021) 158643.
[19] S.G. Tian, Y. Su, B.J. Qian, X.F. Yu, F.S. Liang, A.N. Li, Creep behavior of a single crystal nickel-based superalloy containing 4.2% Re, Mater. Des. 37 (2012) 236–242.
[20] X.X. Wu, S.K. Makineni, C.H. Liebscher, G. Dehm, J. Rezaei Mianroodi, P. Shanthraj, B. Svendsen, D. Bürger, G. Eggeler, D. Raabe, B. Gault, Unveiling the Re effect in Ni-based single crystal superalloys, Nat. Commun. 11 (1) (2020) 389.
[21] W.P. Wu, B. Chen, H.F. Shen, Z.J. Ding, Molecular dynamics simulation of rhenium effects on creep behavior of Ni-based single crystal superalloys, Prog. Nat. Sci. Mater. Int. 32 (2) (2022) 259–266.
[22] K. Durst, M. Göken, Micromechanical characterization of the influence of rhenium on the mechanical properties in nickel-base superalloys, Mater. Sci. Eng., A 387–389 (2004) 312–316.
[23] G.Q. Zhao, S.G. Tian, S.K. Zhang, N. Tian, L.R. Liu, Deformation and damage features of a Re/Ru-containing single crystal nickel base superalloy during creep at elevated temperature, Prog. Nat. Sci. Mater. Int. 29 (2) (2019) 210–216.
[24] M. Huang, J. Zhu, An overview of rhenium effect in single-crystal superalloys, Rare Met. 35 (2) (2016) 127–139.
[25] T. Jin, W.Z. Wang, X.F. Sun, Z.Q. Hu, Role of rhenium in single crystal Ni-based superalloys, Mater. Sci. Forum 638–642 (2010) 2257–2262.
[26] P. Li, Q.Q. Li, T. Jin, Y.Z. Zhou, J.G. Li, X.F. Sun, Z.F. Zhang, Effect of Re on low-cycle fatigue behaviors of Ni-based single-crystal superalloys at 900°C, Mater. Sci. Eng., A 603 (2014) 84–92.
[27] L. Liu, J. Meng, J.L. Liu, M.K. Zou, H.F. Zhang, X.D. Sun, Y.Z. Zhou, Influences of Re on low-cycle fatigue behaviors of single crystal superalloys at intermediate temperature, J. Mater. Sci. Technol. 35 (9) (2019) 1917–1924.
[28] S. Neumeier, F. Pyczak, M. Göken, The temperature dependent lattice misfit of rhenium and ruthenium containing nickel-base superalloys–experiment and modelling, Mater. Des. 198 (2021) 109362.
[29] H. Long, S. Mao, Y. Liu, Z. Zhang, X. Han, Microstructural and compositional design of Ni-based single crystalline superalloys – A review, J. Alloys Compd. 743 (2018) 203–220.
[30] J.C. Zhang, T.W. Huang, F. Lu, K.L. Cao, D. Wang, J. Zhang, J. Zhang, H.J. Su, L. Liu, The effect of rhenium on the microstructure stability and γ/γ' interfacial characteristics of Ni-based single crystal superalloys during long-term aging, J. Alloys Compd. 876 (2021) 160114.
[31] G.Q. Zhao, S.G. Tian, L.R. Liu, N. Tian, F.W. Jin, Deformation mechanism of single-crystal nickel-based superalloys during ultra-high-temperature creep, Rare Met. Mater. Eng. 51 (1) (2022) 52–59.
[32] D.L. Shu, S.G. Tian, L.R. Liu, B.S. Zhang, N. Tian, Elements distribution and deformation features of a 4.5% Re nickel-based single crystal superalloy during creep at high temperature, Mater. Char. 141 (2018) 433–441.
[33] X.G. Wang, J.L. Liu, T. Jin, X.F. Sun, Y.Z. Zhou, Z.Q. Hu, J.H. Do, B.G. Choi, I. S. Kim, C.Y. Jo, Deformation mechanisms of a nickel-based single-crystal superalloy during low-cycle fatigue at different temperatures, Scr. Mater. 99 (2015) 57–60.
[34] S.G. Tian, X.J. Zhu, J. Wu, H.C. Yu, D.L. Shu, B.J. Qian, Influence of temperature on stacking fault energy and creep mechanism of a single crystal nickel-based superalloy, J. Mater. Sci. Technol. 32 (8) (2016) 790–798.
[35] N. Tian, G.Q. Zhao, T. Meng, S.G. Tian, L.R. Liu, H.J. Yan, G.Y. Wang, F.W. Jin, Ultra-high-temperature creep behavior of a single-crystal nickel-based superalloy containing 6% Re/5% Ru, Mater. Char. 180 (2021) 111394.
[36] Z. Tan, X.G. Wang, Z.C. Ge, Y.H. Mu, Y.M. Li, J.C. Pang, X. Tao, M. Zou, Y. Yang, J. Liu, J. Liu, J. Li, Y. Zhou, X. Sun, Dependence of deformation mechanisms on micro-pores in the fourth-generation single crystal superalloy during out-of-phase thermal-mechanical fatigue, Int. J. Fatig. 180 (2024) 108086.
[37] Z. Tan, C.L. Zou, X.G. Wang, J.C. Pang, Y.M. Li, J.J. Liang, J.D. Liu, J.L. Liu, J.G. Li, Z.F. Zhang, X.F. Sun, Y.Z. Zhou, Micro-scale local damage mechanisms and life prediction method of the fourth-generation single crystal superalloy under thermal-mechanical fatigue, Scr. Mater. 269 (2025) 116935.
[38] R.Q. Wang, K.H. Jiang, F.L. Jing, D.Y. Hu, Thermomechanical fatigue failure investigation on a single crystal nickel superalloy turbine blade, Eng. Fail. Anal. 66 (2016) 284–295.
[39] W.P. Wu, Y.F. Guo, Y.S. Wang, Evolution of misfit dislocation network and tensile properties in Ni-based superalloys: a molecular dynamics simulation, Sci. China Phys. Mech. Astron. 55 (3) (2012) 419–427.

[40] N.L. Li, W.P. Wu, K. Nie, Molecular dynamics study on the evolution of interfacial dislocation network and mechanical properties of Ni-based single crystal superalloys, Phys. Lett. 382 (20) (2018) 1361–1367.
[41] B. Chen, W.P. Wu, Molecular dynamics simulations of dynamics mechanical behavior and interfacial microstructure evolution of Ni-based single crystal superalloys under shock loading, J. Mater. Res. Technol. 15 (2021) 6786–6796.
[42] J.P. Wang, J.W. Liang, Z.X. Wen, Z.F. Yue, Y. Peng, Unveiling the local deformation behavior of typical microstructures of nickel-based single crystals under nanoindentation, Mech. Mater. 166 (2022) 104204.
[43] B. Chen, W.P. Wu, M.X. Chen, Orientation dependence of microstructure deformation mechanism and tensile mechanical properties of nickel-based single crystal superalloys: a molecular dynamics simulation, Comput. Mater. Sci. 202 (2022) 111015.
[44] B. Chen, Y.L. Li, D. Sopu, J. Eckert, W.P. Wu, Molecular dynamics study of shock-induced deformation phenomena and spallation failure in Ni-based single crystal superalloys, Int. J. Plast. 162 (2023) 103539.
[45] W.P. Wu, Z.J. Ding, B. Chen, H.F. Shen, Y.L. Li, Effect of rhenium on low cycle fatigue behaviors of Ni-based single crystal superalloys: a molecular dynamics simulation, J. Mater. Res. Technol. 18 (2022) 5144–5160.
[46] B. Chen, W.P. Wu, M.X. Chen, Y.F. Guo, Molecular dynamics study of fatigue mechanical properties and microstructural evolution of Ni-based single crystal superalloys under cyclic loading, Comput. Mater. Sci. 185 (2020) 109954.
[47] W.P. Wu, Z.J. Ding, Y.L. Li, C. Yu, G.Z. Kang, Molecular dynamics simulation of thermomechanical fatigue properties of Ni-based single crystal superalloys, Int. J. Fatig. 173 (2023) 107667.
[48] R.C. Reed, T. Tao, N. Warnken, Alloys-by-design: application to nickel-based single crystal superalloys, Acta Mater. 57 (19) (2009) 5898–5913.
[49] M. Ramsperger, R.F. Singer, C. Körner, Microstructure of the nickel-base superalloy CMSX-4 fabricated by selective electron beam melting, Metall. Mater. Trans. 47 (2016) 1469–1480.
[50] K.P.L. Fullagar, R.W. Broomfield, M. Hulands, K. Harris, G.L. Erickson, S. L. Sikkenga, Aero engine test experience with CMSX-4® alloy single-crystal turbine blades, J. Eng. Gas Turbines Power 118 (2) (1996) 380–388.
[51] S.J. Plimpton, Fast parallel algorithms for short-range molecular dynamics, J. Comput. Phys. 117 (1995) 1–19. http://lammps.sandia.gov/.
[52] T. Zhu, C.Y. Wang, Molecular dynamics study of mosaic structure in the Ni-based single-crystal superalloy, Chin. Phys. 15 (9) (2006) 2087–2091.
[53] Y.M. Li, X.G. Wang, Z.H. Tan, J.D. Liu, J.L. Liu, J.G. Li, Y.Z. Zhou, X.F. Sun, On dislocation networks and superdislocations in Re-containing nickel-based SX superalloy under different creep conditions, Intermetallics 148 (2022) 107646.
[54] S. Neumeier, F. Pyczak, M. Göken, Influence of rhenium and ruthenium on the local mechanical properties of the γ and γ' phases in nickel-base superalloys, Philos. Mag. 91 (33) (2011) 4187–4199.
[55] S. Tian, X. Meng, Z. Zeng, C. Zhang, C. Liu, Influence of element Re on creep behavior of single crystal nickel-based superalloys at intermediate temperature, High Temp. Mater. Process. 32 (1) (2013) 7–13.
[56] T.M. Pollock, S. Tin, Nickel-based superalloys for advanced turbine engines: chemistry, microstructure and properties, J. Propul. Power 22 (2) (2006) 361–374.
[57] E. Fleischmann, M.K. Miller, E. Affeldt, U. Glatzel, Quantitative experimental determination of the solid solution hardening potential of rhenium, tungsten and molybdenum in single-crystal nickel-based superalloys, Acta Mater. 87 (2015) 350–356.
[58] J.P. Du, C.Y. Wang, T. Yu, Construction and application of multielement EAM potential (Ni-Al-Re) in γ/γ' Ni-based single crystal superalloys, Model. Simulat. Mater. Sci. Eng. 21 (1) (2013) 015007.
[59] Q. Yin, R.H. Wu, J.P. Wang, S.Q. Chen, Y.D. Lian, Z.X. Wen, Elastoplastic behavior of the γ-phase in Ni-based single crystal superalloys: a molecular dynamics study considering Re and temperature effect, Mech. Mater. 160 (2021) 103989.
[60] D. Faken, H. Jónsson, Systematic analysis of local atomic structure combined with 3D computer graphics, Comput. Mater. Sci. 2 (2) (1994) 279–286.
[61] A. Stukowski, V.V. Bulatov, A. Arsenlis, Automated identification and indexing of dislocations in crystal interfaces, Model. Simulat. Mater. Sci. Eng. 20 (8) (2012) 085007.
[62] A. Stukowski, Visualization and analysis of atomistic simulation data with OVITO–the Open visualization Tool, Model. Simulat. Mater. Sci. Eng. 18 (1) (2010) 015012.
[63] J.J. Yang, F.L. Jing, Z.M. Yang, K.H. Jiang, D.Y. Hu, B. Zhang, Thermomechanical fatigue damage mechanism and life assessment of a single crystal Ni-based superalloy, J. Alloys Compd. 872 (2021) 159578.
[64] J.J. Moverare, S. Johansson, R.C. Reed, Deformation and damage mechanisms during thermal–mechanical fatigue of a single-crystal superalloy, Acta Mater. 57 (7) (2009) 2266–2276.
[65] Z.X. Shi, S.Z. Liu, X.G. Wang, X.D. Yue, J.R. Li, Effect of melting temperature on the microstructure stability of a Ni-based single crystal superalloy, Procedia Eng. 99 (2015) 1415–1420.
[66] D.M. Li, W.J. Nam, C.S. Lee, A strain energy-based approach to the low-cycle fatigue damage mechanism in a high-strength spring steel, Metall. Mater. Trans. 29 (5) (1998) 1431–1439.
[67] J. Yu, G. Han, Z. Chu, X. Sun, T. Jin, Z. Hu, High temperature thermo-mechanical and low cycle fatigue behaviors of DD32 single crystal superalloy, Mater. Sci. Eng., A 592 (2014) 164–172.
[68] A. Mottura, R.T. Wu, M.W. Finnis, R.C. Reed, A critique of rhenium clustering in Ni–Re alloys using extended X-ray absorption spectroscopy, Acta Mater. 56 (11) (2008) 2669–2675.
[69] A. Mottura, N. Warnken, M.K. Miller, M.W. Finnis, R.C. Reed, Atom probe tomography analysis of the distribution of rhenium in nickel alloys, Acta Mater. 58 (3) (2010) 931–942.
[70] K.T. Butler, G.S. Gautam, P. Canepa, Designing interfaces in energy materials applications with first-principles calculations, npj Comput. Mater. 5 (2019) 19.
[71] W.J. Ostergren, A damage function and associated failure equations for predicting hold time and frequency effects in elevated temperature, low cycle fatigue, J. Test. Eval. 4 (1976) 327–339.